JOURNAL OF SPACECRAFT AND ROCKETS
Vol. 29, No. 2, March-April 1992

Sensor Placement for On-Orbit Modal Testing

Tae W. Lim*
Lockheed Engineering and Sciences Company, Hampton, Virginia 23666

A systematic procedure of placing sensors for the on-orbit modal identification of large flexible space structures is addressed. The concepts of system and component modal costs are introduced as a means of selecting target modes for modal testing. Assuming that a time-domain modal identification algorithm is employed to identify the modes from measured time response data, the sensors are placed to enhance the recovery of the target modes. As an application example of the procedure, an accelerometer placement study for the Space Station Freedom On-Orbit Modal Identification Experiment is presented.

Introduction

ON-ORBIT identified modal characteristics of a large space structure such as Space Station Freedom (SSF) are essential in validating the finite element model of the structure, since a ground modal test of the structure is not feasible due to its size and flexibility. The validated finite element model will be valuable in performing structural dynamic analyses and control system syntheses. Issues pertaining to on-orbit modal identification have been studied under a program called the SSF On-Orbit Modal Identification Experiment (MIE).[1-4] One of the issues is the placement of sensors (accelerometers) on the structure to enhance the modal identification of target modes. Since the performance of modal parameter identification algorithms depends on measured response data, a systematic sensor placement method to obtain best measurement data is needed. The placement of sensors should be evaluated under the constraints of the on-orbit modal testing environment, including a limited number of sensors due to weight and cost, limited excitation sources, limited locations to place sensors, and limited sensor movement or replacement.

Sensor placement techniques for structural parameter identification have been addressed by Shah and Udwadia,[5] Salama et al.,[6] and Kammer.[7] However, sensor placement in conjunction with the performance of modal parameter identification algorithms has not been addressed. In this paper, assuming that a time-domain modal identification algorithm, eigensystem realization algorithm (ERA),[8] is employed for on-orbit modal identification, a sensor placement procedure to enhance the modal identification of target modes is addressed. The generalized Hankel matrix used in ERA is a product of the controllability and observability matrices. The rank of the Hankel matrix is generally a measure of the number of modes in a structural system and depends on the minimum rank of the controllability and observability matrices. Since excitation locations for on-orbit modal testing are assumed fixed, the rank of the controllability matrix is given. Thus, the problem may be stated as follows: place a number of sensors to obtain the desired rank of the observability matrix while satisfying given on-orbit modal testing constraints. The effective independence (EI) approach proposed by Kammer[7] is employed to rank candidate sensor locations according to the contribution to the linear independence of the target modes. Sensor locations contributing insignificantly are removed in an iterative manner until a small number of best sensor locations is obtained.

This paper also addresses important issues such as the selection procedures for the target modes and the candidate sensor locations, and sensor redundancy management. An accelerometer placement study for the MIE is presented as an application example of the procedure.

Selection of Target Modes

Modal properties of large flexible space structures are characterized by closely spaced modes with high modal density. Identification of all of the modes within a certain frequency band would require freedom in moving and adding excitation sources because a limited number of modes would be excited properly at a given excitation location. However, excitation sources for on-orbit modal testing are often fixed at specified locations. Also, the magnitude and the type of forcing function that the excitation sources can generate are limited. Therefore, it is expected that a subset of the modes would be excited properly. The modes excited properly by the excitation sources at specified locations are referred to as "excitable modes."

A large space structure is typically composed of various components with distinctive dynamic characteristics. Because of the complexity of the structure, many of the modes represent local motion confined to particular components rather than the global motion of the entire structure. Individual components may have been validated through ground modal testing and may not be of strong interest for on-orbit modal testing. Thus, it would be necessary to select the excitable modes representing the global motion of the entire structure. These modes are referred to as "target modes," and the design of on-orbit modal testing is tailored to identify them. The performance of identifying the target modes is an important indicator in evaluating the effectiveness of a modal testing design. A procedure of selecting the target modes is addressed here.

Using the finite element method, the equation of motion governing the response of lightly damped large space structures is represented by

$$M\ddot{u} + C\dot{u} + Ku = Ff \tag{1}$$

where the matrices M, C, and K are $n \times n$ damping, and stiffness matrices, respectively; u and f are an $n \times 1$ displacement vector and an $n_f \times 1$ excitation vector, respectively: a force distribution matrix F is used to define excitation locations in the equation. Employing the transformation of $u = \Phi q$ and assuming that the damping matrix is proportional, Eq. (1) can be rewritten in the modal coordinates as

$$\ddot{q} + 2Z\Omega\dot{q} + \Omega^2 q = \Phi^T F f = Ef \tag{2}$$

Presented as Paper 91-1184 at the AIAA/ASME/ASCE/AHS/ASC 32nd Structures, Structural Dynamics, and Materials Conference, Baltimore, MD, April 8-10, 1991; received April 26, 1991; revision received Sept. 5, 1991; accepted for publication Sept. 9, 1991.

*Senior Engineer, Langley Program Office, 144 Research Drive. Member AIAA.

where $Z = \text{diag}\{\zeta_i\}$ and $\Omega = \text{diag}\{\omega_i\}$; Φ is an $n \times n_m$ modal matrix normalized to yield the unit generalized mass, and q represents the displacement in the modal coordinates. The quantity n_m is the number of the modes used in the transformation. In general, an n_y dimensional measurement vector is defined as

$$y = Y_d q + Y_v \dot{q} + Df \tag{3}$$

where Y_d, Y_v, and D are the matrices with appropriate dimensions, and they depend on the types and locations of the measurement vector.

When a structure is excited, the kinetic and strain energy is distributed among the components of the structure. The kinetic energy T_{ij} and strain energy V_{ij} for mode i and component j are evaluated by

$$T_{ij} = \tfrac{1}{2}\phi_i^T M_j \phi_i \dot{q}_i^2 = \tfrac{1}{2} m_{ij} \dot{q}_i^2 \tag{4}$$

$$V_{ij} = \tfrac{1}{2}\phi_i^T K_j \phi_i q_i^2 = \tfrac{1}{2} k_{ij} \omega_i^2 q_i^2 \tag{5}$$

where M_j and K_j are the mass and stiffness matrices for the component j; ϕ_i is the ith mode shape vector; and $m_{ij} = \phi_i^T M_j \phi_i$ and $k_{ij}\omega_i^2 = \phi_i^T K_j \phi_i$ ($0 \le m_{ij} \le 1$ and $0 \le k_{ij} \le 1$). The kinetic energy T and strain energy V of the entire structure become

$$T = \sum_{i=1}^{n_m}\sum_{j=1}^{n_c} T_{ij} = \tfrac{1}{2}\sum_{i=1}^{n_m}\sum_{j=1}^{n_c} m_{ij}\dot{q}_i^2 = \tfrac{1}{2}\sum_{i=1}^{n_m} \dot{q}_i^2 \tag{6}$$

$$V = \sum_{i=1}^{n_m}\sum_{j=1}^{n_c} V_{ij} = \tfrac{1}{2}\sum_{i=1}^{n_m}\sum_{j=1}^{n_c} k_{ij}\omega_i^2 q_i^2 = \tfrac{1}{2}\sum_{i=1}^{n_m} \omega_i^2 q_i^2 \tag{7}$$

where the quantity n_c is the number of the components.

Assume that a zero-mean, unit-intensity white noise disturbance is applied as excitation and that the displacement and velocity measurements are made in the modal coordinates. For the entire structure, the system modal cost of mode i to minimize a cost measure

$$J = \lim_{t\to\infty} E(T + V) \tag{8}$$

where, from Eqs. (6) and (7),

$$T + V = \sum_{i=1}^{nm}\left(\tfrac{1}{2}\sum_{j=1}^{nc} m_{ij}\dot{q}_i^2 + \tfrac{1}{2}\sum_{i=1}^{nc} k_{ij}\omega_i^2 q_i^2\right) \tag{9}$$

is approximated by[9]

$$\mu_i = \tfrac{1}{2}\left(\sum_{j=1}^{n_c}[m_{ij} + k_{ij}]\right) e_i e_i^T/(4\zeta_i\omega_i) = e_i e_i^T/(4\zeta_i\omega_i) \tag{10}$$

where e_i is the ith row of matrix E in Eq. (2). The system modal cost indicates the effort required to dissipate energy contained in the individual modes. Thus, the modes with higher modal cost will be easier to excite and vice versa. The excitable modes are defined as the minimum number of modes that satisfy

$$\sum_{i=1}^{n_e} \hat{\mu}_i > \alpha\mu_{\text{total}} = \alpha\sum_{i=1}^{n_m}\mu_i \tag{11}$$

where $\hat{\mu}_i$ indicates the system modal cost sorted in a descending order and n_e is the number of excitable modes. The quantity α indicates a fraction of the total modal cost. For example, when $\alpha = 0.95$, the modes accounting for 95% of the total system modal cost will be selected.

As described previously, the excitable modes may contain local modes confined to components. The global system modes are extracted from the excitable modes as the target modes. For instance, the backbone of the SSF structure as shown in Fig. 1 is a truss assembly. The truss assembly provides structure to support a module cluster, photovoltaic (PV) arrays, thermal radiators, and various payloads. Ground modal testing of the truss assembly will not be feasible due to its size and flexibility. Thus the modes associated with the truss assembly are defined as the global modes. From Eq. (10), the component modal cost for component j and mode i is easily derived as

$$\mu_{ij} = (m_{ij} + k_{ij}) e_i e_i^T/(8\zeta_i\omega_i) \tag{12}$$

Therefore, the target modes for component j are the minimum number of modes among the excitable modes that satisfy

$$\sum_{i=1}^{n_{tj}} \hat{\mu}_{ij} > \beta_j \sum_{i=1}^{n_e}\mu_{ij} \tag{13}$$

where $\hat{\mu}_{ij}$ indicates the component modal cost sorted in a descending order and n_{tj} is the number of target modes for component j. The quantity β_j indicates a fraction of the total modal cost for component j among the excitable modes.

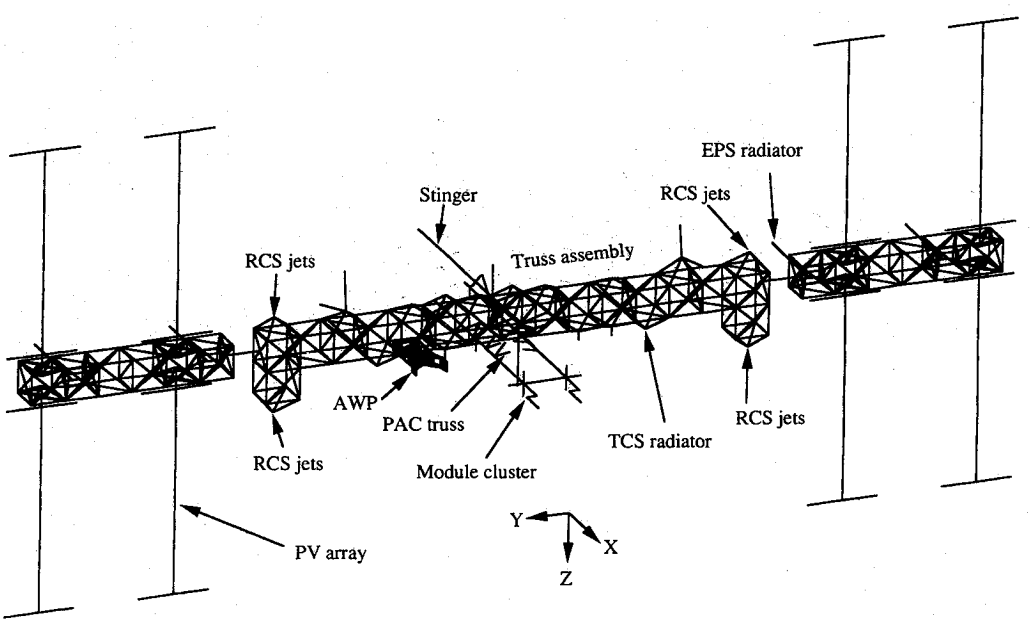

Fig. 1 Finite element model of SSF assembly complete configuration.[10]

Selection of Candidate Sensor Locations

Installation of accelerometers at all of the finite element degrees of freedom (DOF) is not feasible due to cost, limited accessibility, inadequacy of mounting locations, and operation and maintenance constraints of a space structure. These data on the feasible sensor locations are incorporated in selecting candidate sensor locations. The candidate sensor locations are also selected to represent all major components in a structural system. The component modal cost distribution among the target modes can be used to identify important components that need instrumentation.

Procedure for Sensor Placement

The procedure of defining target modes and the guidelines of selecting candidate sensor locations have been addressed. Now the task is to select the best sensor locations to enhance the identification of the target modes, assuming that the time domain modal identification algorithm, ERA, is employed for modal parameter identification.

Theoretical Background

Define a state vector $x = \{q^T \dot{q}^T\}^T$. Then an equivalent state-space representation of Eqs. (2) and (3) is obtained as

$$\dot{x} = \hat{A}x + \hat{B}f \tag{14}$$

$$y = Cx + Df \tag{15}$$

where

$$\hat{A} = \begin{bmatrix} 0 & I \\ -\Omega^2 & -2Z\Omega \end{bmatrix}, \qquad \hat{B} = \begin{bmatrix} 0 \\ E \end{bmatrix}, \qquad C = [Y_d \;\; Y_v] \tag{16}$$

Since accelerometers are used to measure the response, the matrices in Eqs. (15) and (16) become

$$Y_d = -Y\Phi\Omega^2 = -\Phi_y\Omega^2 \tag{17}$$

$$Y_v = -2Y\Phi Z\Omega = -2\Phi_y Z\Omega \tag{18}$$

$$D = Y\Phi E = \Phi_y E \tag{19}$$

where the matrix Y contains the information on the measurement locations. Discretize Eqs. (14) and (15) to obtain for $k = 0, 1, 2, \ldots$

$$x(k+1) = Ax(k) + Bf(k) \tag{20}$$

$$y(k) = Cx(k) + Df(k) \tag{21}$$

where

$$A = e^{\hat{A}h}, \qquad B = \left(\int_0^h e^{\hat{A}T}\, dT\right)\hat{B}$$

and h = time step.

The eigensystem realization algorithm forms a generalized Hankel matrix that is a product of the observability and controllability matrices. The generalized Hankel matrix $H_{rs}(0)$ is written as

$$H_{rs}(0) = V_r W_s \tag{22}$$

The matrices V_r and W_s are the observability and controllability matrices, respectively, and are defined as

$$V_r = \begin{bmatrix} C \\ CA^{j_1} \\ \cdot \\ \cdot \\ CA^{j_{r-1}} \end{bmatrix}, \qquad W_s = [B \;\; A^{t_1}B \;\; \ldots \;\; A^{t_{s-1}}B] \tag{23}$$

where j_i $(i = 1, \ldots, r-1)$ and t_i $(i = 1, \ldots, s-1)$ are arbitrary integers. The singular value decomposition is performed on the Hankel matrix $H_{rs}(0)$, and the number of modes identified depends on the rank of the Hankel matrix. The rank of $H_{rs}(0)$ is

$$\rho[H_{rs}(0)] \le \min[\rho(V_r), \rho(W_s)] \tag{24}$$

where $\rho(.)$ represents the rank of a matrix.

Since the excitation locations for on-orbit modal testing are assumed fixed at specified locations, matrix B in Eq. (23) is given. Assume that the target modes were used solely to define matrix A. If the rank of the controllability matrix with given A and B matrices is smaller than $2n_t$ (n_t = the number of target modes), the rank of the Hankel matrix will be smaller than $2n_t$ and the complete identification of all of the target modes will not be possible regardless of sensor locations. Therefore, once excitation locations and target modes are defined, the rank of the controllability matrix should be examined to ensure that all of the target modes are excitable. By selecting the excitable modes (i.e., controllable modes) as the target modes, the problem of having a rank deficient controllability matrix can be avoided.

When a structure is excited, all of the excitable modes participate in the response. An accurate representation of input-output behavior of the structure will be obtained by incorporating all of the excitable modes into Eq. (20). In this case, the rank of matrix A becomes $2n_e$. If $j_i = i$ $(i = 1,2, \ldots)$ is used, the rank of the observability matrix V_r can be evaluated by examining the rank of a matrix[11]

$$Q = \begin{bmatrix} C \\ CA \\ \cdot \\ \cdot \\ CA^{\rho(A)-\rho(C)} \end{bmatrix} \tag{25}$$

The output equation, Eq. (21), can be rewritten by considering the partition of the target modes and the nontarget modes among the excitable modes

$$y(k) = [C_t \;\; C_n] \begin{Bmatrix} x_t(k) \\ x_n(k) \end{Bmatrix} + Df(k) \tag{26}$$

where the subscripts t and n indicate the target mode set and the nontarget mode set, respectively. Since matrix Φ_y is assumed nonsingular, the ranks of the matrices C_t and C_n become, from Eqs. (16-18),

$$\rho(C_t) = \rho(\Phi_{yt}) = \min(n_s, n_t) \tag{27}$$

$$\rho(C_n) = \rho(\Phi_{yn}) = \min(n_s, n_n) \tag{28}$$

respectively, where n_s is the number of sensors, n_n is the number of the nontarget modes, and $n_e = n_t + n_n$. Assuming that the response contribution from the nontarget modes is insignificant, replace C with C_t in matrix Q in Eq. (25). Then the rank of matrix Q_t is bounded by

$$\rho(C_t) \le \rho(Q_t) \le 2n_e \tag{29}$$

where Q_t is the matrix Q with C replaced by C_t. Thus, the lower bound of $\rho(Q_t)$ depends on $\min(n_s, n_t)$.

Considering that the primary goal of on-orbit modal testing is to identify the target modes, $\rho(Q_t)$ should be at least $2n_t$ and the identification should include all of the target modes. Equation (29) does not provide an absolute indication as to the minimum number of sensors required to identify all of the target modes. The lower bound of $\rho(Q_t)$ can be maintained at n_t by having at least as many sensors as the number of target modes, i.e., $n_s = n_t$, and keeping the full rank of matrix Φ_{yt}. There may be many sets of sensor locations satisfying

$\rho(\Phi_{yt}) = n_t$ with $n_s = n_t$. A reasonable choice (but not the only one) of the best set could be made by selecting the one with the would allow best possible distinction of the mode shapes of the target modes and hence enhance the modal identification performance. Therefore, the sensor placement problem is stated as follows: select at least n_t number of sensor locations that minimize cond(Φ_{yt}) among the candidate sensor locations. Though the n_t number of sensor locations selected to minimize cond(Φ_{yt}) does not guarantee complete identification of all of the target modes, these sensor locations contain vital response information and are crucial in distinguishing the target modes.

Implementation of the Procedure

The EI approach proposed by Kammer[7] is employed to select the sensor locations that minimize cond(Φ_{yt}). This approach provides an efficient suboptimal procedure to reduce the number of candidate sensors without significantly deteriorating cond(Φ_{yt}) by removing less effective candidate sensor locations. The contribution of the ith row of the matrix Φ_{yt}, i.e., the ith candidate sensor DOF, to the linear independence of the matrix is evaluated by

$$E_i = [\text{diag}(\Phi_{yt}\Phi_{yt}^{+})]_i \tag{30}$$

where E_i is the EI value of the ith row of Φ_{yt} and + represents a pseudoinverse. In an iterative manner, the rows contributing little to the effective independence are removed from the matrix until a desired number of rows remains. The sensor locations corresponding to the remaining rows are the best locations.

Though the suggested minimum number of sensors is equal to the number of target modes, in practice more sensors will be required for the following reasons: 1) The target mode selection procedure and the sensor placement procedure depend solely on the analytical estimation of the structure. 2) For the correlation of the analytical and experimental mode shapes and the analytical model improvement using test data, more information on the mode shapes is generally required.

The sensor placement is performed using the mode shape information of the target modes. When the modal cost of the nontarget modes is large, it is possible to have sensor locations where the response contribution from the nontarget modes is significant. This observation "spillover" may cause inaccuracy in the identification of the target modes. The spillover can be prevented by examining the EI distribution of the nontarget modes and removing the candidate sensor locations with relatively large nontarget mode EI values compared with target mode EI values.

Once the sensors are in place, they are expected to provide measurement information during a series of on-orbit modal tests. Some sensors may need backup sensors to protect the crucial measurement information. Since the EI value of a sensor indicates the cost of losing the sensor, the sensors with large EI values should be provided with redundancy. The minimum number of sensors is equal to the number of target modes to be identified. Therefore, a reasonable approach is to provide redundancy for the minimum number of sensors with the largest EI values.

Application Example: Sensor Placement Study for Space Station Freedom Modal Identification Experiment

Sensor placement for the MIE is investigated using the proposed procedure. The finite element model of the SSF assembly complete configuration shown in Fig. 1 is used for the study. The excitation for on-orbit modal testing is provided in the X and Z directions by the reaction control system (RCS) jets located on the truss assembly as indicated in the figure. The locations of the jets are fixed. The configuration has 108 modes below 2 Hz including 6 rigid body modes.

Selection of the Target Modes

The modal cost of the entire system is valued to extract the excitable modes using the RCS jets. The modal cost of the entire system is shown in Fig. 2. Thirty modes that account for about 95% of the total modal cost are selected as the excitable modes and listed in Table 1. To extract the global system modes from the excitable modes, the assembly complete configuration is decomposed into eight components: 1) truss assembly, 2) module cluster, 3) PV arrays, 4) electric power system (EPS) radiators, 5) thermal control system (TCS) radiators, 6) assembly work platform (AWP), 7) module support truss (PAC truss), and 8) stinger. The modal cost of each component is calculated and shown in Table 1 for the excitable modes. Among the excitable modes, 18 modes that account for about 95% of the modal cost in the truss assembly component are selected as the target modes (bold faced). Among the excitable modes, the total system modal cost of the nontarget modes is less than 8% of that of the target modes. Thus, the measurement spillover from the nontarget modes is expected to be small.

Many of the target modes exhibit strong coupling with other components. For instance, the modal cost of mode 21 in the truss assembly is comparable to that in the PV arrays. Module cluster, PV arrays, EPS radiators, TCS radiators, and stinger show significant shares of modal cost among the target modes. This indicates that instrumentation of those components will facilitate the characterization and modal identification of the target modes.

To ensure that all of the target modes are excitable, the rank of the controllability matrix W_s in Eq. (23) using all 18 target modes and all 8 excitation DOF was evaluated using the singular value decomposition. The rank of the matrix was 36, indicating that all 18 target modes are excitable. The condition number obtained, which is the ratio of the maximum and minimum singular values, was 89.4, indicating a good linear independence of the target modes with respect to the excitation location DOF. The proposed target mode selection procedure ensures that all of the target modes are excitable.

Selection of the Candidate Sensor Locations

Based on the guidelines mentioned previously, candidate sensor locations (326 DOF) are selected and shown in Fig. 3 and Table 2. To save extravehicular activity time and cost of installing sensors and to enhance the modal identification of individual components, a group of sensors is considered as a unit. The sensor placement is made based on the performance

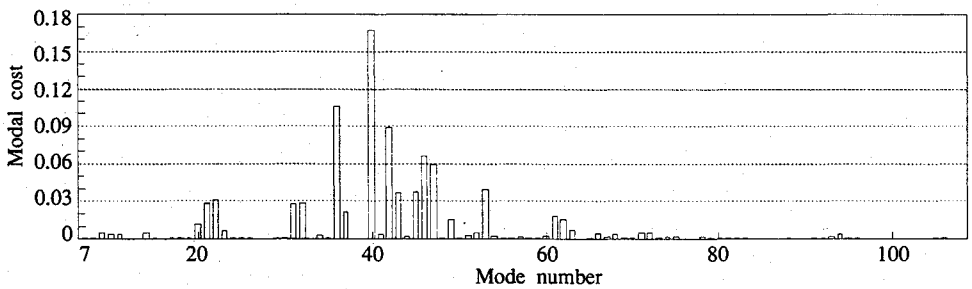

Fig. 2 Modal cost of the entire system.

Table 1 Distribution of component modal cost among the excitable modes[a]

Mode number	Freq., Hz	Truss assembly	Module cluster	PV arrays	EPS radiators	TCS radiators	AWP	PAC truss	Stinger	Total system
9	0.091	0.00032	0.00000	0.00395	0.00033	0.00000	0.00000	0.00000	0.00000	0.00460
10	0.092	0.00029	0.00008	0.00043	0.00262	0.00000	0.00000	0.00001	0.00000	0.00343
11	0.094	0.00032	0.00005	0.00252	0.00043	0.00000	0.00000	0.00000	0.00000	0.00333
14	0.096	0.00005	0.00000	0.00040	0.00467	0.00000	0.00000	0.00000	0.00000	0.00512
20	0.100	0.00024	0.00007	0.01116	0.00001	0.00001	0.00000	0.00001	0.00000	0.01150
21	**0.115**	**0.01303**	**0.00097**	**0.01186**	**0.00211**	**0.00008**	**0.00000**	**0.00007**	**0.00000**	**0.02814**
22	**0.131**	**0.01181**	**0.00104**	**0.00286**	**0.00026**	**0.01448**	**0.00000**	**0.00011**	**0.00000**	**0.03059**
23	0.133	0.00020	0.00001	0.00583	0.00000	0.00001	0.00000	0.00000	0.00000	0.00605
31	**0.139**	**0.01027**	**0.00098**	**0.00174**	**0.00024**	**0.01412**	**0.00000**	**0.00009**	**0.00000**	**0.02747**
32	**0.148**	**0.00936**	**0.00119**	**0.01712**	**0.00035**	**0.00011**	**0.00001**	**0.00006**	**0.00000**	**0.02823**
36	**0.286**	**0.03971**	**0.04578**	**0.00553**	**0.00029**	**0.00539**	**0.00021**	**0.00877**	**0.00046**	**0.10621**
37	**0.326**	**0.01044**	**0.00702**	**0.00066**	**0.00007**	**0.00026**	**0.00017**	**0.00234**	**0.00002**	**0.02099**
40	**0.401**	**0.13975**	**0.00383**	**0.00764**	**0.00206**	**0.00901**	**0.00064**	**0.00439**	**0.00007**	**0.16750**
41	0.427	0.00014	0.00355	0.00001	0.00000	0.00000	0.00000	0.00000	0.00000	0.00371
42	**0.457**	**0.04882**	**0.03026**	**0.00203**	**0.00108**	**0.00099**	**0.00021**	**0.00343**	**0.00225**	**0.08913**
43	**0.479**	**0.01327**	**0.00060**	**0.00054**	**0.00047**	**0.00063**	**0.00004**	**0.00093**	**0.01970**	**0.03620**
45	**0.489**	**0.01710**	**0.00418**	**0.00092**	**0.00053**	**0.00073**	**0.00005**	**0.00287**	**0.01086**	**0.03726**
46	**0.491**	**0.04126**	**0.00546**	**0.00217**	**0.00212**	**0.00022**	**0.00017**	**0.00403**	**0.01074**	**0.06619**
47	**0.560**	**0.04195**	**0.00336**	**0.00173**	**0.00998**	**0.00016**	**0.00008**	**0.00169**	**0.00014**	**0.05911**
49	**0.589**	**0.00318**	**0.00096**	**0.00010**	**0.01013**	**0.00004**	**0.00000**	**0.00024**	**0.00000**	**0.01467**
52	0.598	0.00030	0.00006	0.00002	0.00436	0.00001	0.00000	0.00003	0.00000	0.00477
53	**0.618**	**0.02133**	**0.00468**	**0.00114**	**0.01025**	**0.00052**	**0.00002**	**0.00071**	**0.00003**	**0.03870**
61	**0.904**	**0.01010**	**0.00270**	**0.00021**	**0.00241**	**0.00095**	**0.00001**	**0.00185**	**0.00007**	**0.01831**
62	**1.003**	**0.00811**	**0.00089**	**0.00031**	**0.00018**	**0.00538**	**0.00004**	**0.00022**	**0.00000**	**0.01514**
63	**1.055**	**0.00324**	**0.00042**	**0.00008**	**0.00007**	**0.00251**	**0.00002**	**0.00019**	**0.00001**	**0.00654**
66	1.114	0.00288	0.00066	0.00006	0.00004	0.00057	0.00018	0.00011	0.00000	0.00450
68	1.240	0.00263	0.00019	0.00005	0.00014	0.00023	0.00004	0.00014	0.00003	0.00345
71	1.313	0.00265	0.00005	0.00015	0.00161	0.00005	0.00000	0.00000	0.00000	0.00452
72	1.320	0.00281	0.00022	0.00014	0.00161	0.00017	0.00000	0.00002	0.00001	0.00498
94	**1.790**	**0.00303**	**0.00008**	**0.00001**	**0.00000**	**0.00004**	**0.00006**	**0.00007**	**0.00000**	**0.00329**

[a]Boldface numbers indicate the target modes for the truss assemby.

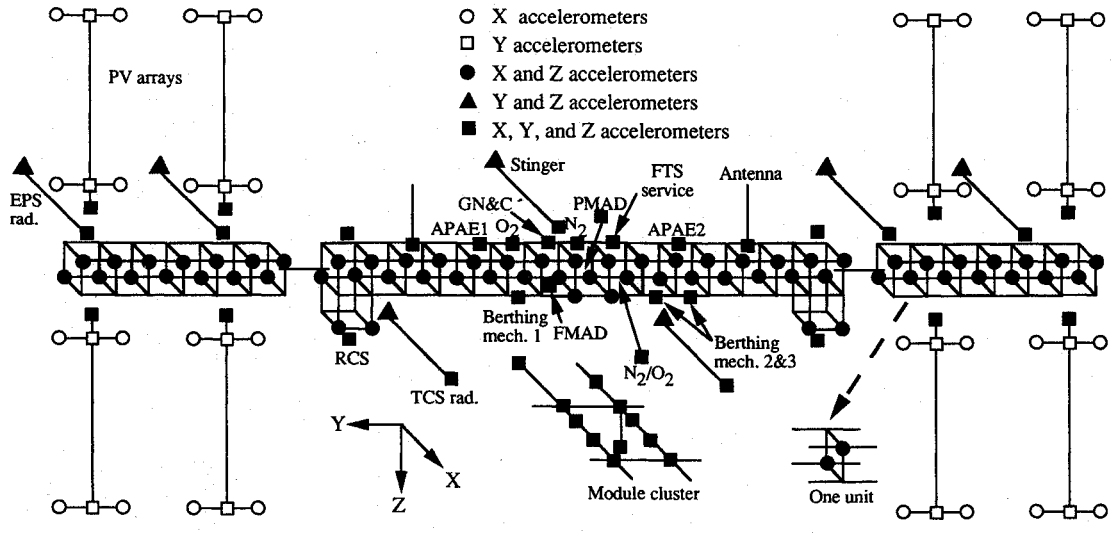

Fig. 3 Candidate sensor locations.

as a unit. Seventy-four sensor units are defined and shown in Table 2. As shown in Fig. 3, the sensors placed in a bay of the truss assembly are considered as a unit. The sensors on each PV array are a unit. The sensors located on each radiator and stinger are a unit. Each triaxial accelerometer located on the module cluster, the pallets, and various nodes are considered as a unit.

Placement of Sensors

The best sensor units to identify the 18 target modes are investigated using the EI approach. Figure 4a shows the initial evaluation of the average EI value of each unit. The average EI value of each unit indicates collectively the effectiveness of the individual accelerometers in the unit. The contribution from the radiator and stinger sensor units is prominent. This is expected since the target modes have strong coupling with the radiators, stinger, and PV arrays as shown in Table 1. A couple of units with the smallest EI values are removed in each iteration until a "reasonable" number of units remains. The reasonable number of units is determined to maintain spatial distribution of sensors on the truss assembly. The final evaluation of EI values is shown in Fig. 4b. Out of 74 candidate sensor units, 26 units remain, indicating the best locations for sensor placement. The best 26 units (133 DOF) are shown in Fig. 5. Some modal identification algorithms require the driving point measurements. In this case, the upper RCS jet locations need to be instrumented as well.

The EI distribution of the nontarget modes among the candidate sensor units is evaluated to examine the influence of the nontarget modes. Figure 6 shows the ratios between the

Table 2 Summary of the candidate sensor locations

Locations	Number of sensors in DOF	Number of sensors in units
Truss assembly	$24 \times (XZ + XZ) = 96$	30
	$6 \times (XZ + XZ + XZ) = 36$	
PV arrays	$8 \times (4X + 2Y + XYZ) = 72$	8
Module cluster	$11 \times (XYZ) = 33$	11
EPS radiators	$4 \times (YZ + XYZ) = 20$	4
TCS radiators	$2 \times (YZ + XYZ) = 10$	2
Stinger	$YZ + XYZ = 5$	1
RCS pallets	$4 \times (XYZ) = 12$	4
GN&C pallet	$XYZ = 3$	1
PMAD pallet	$XYZ = 3$	1
FMAD pallet	$XYZ = 3$	1
APAE pallets	$2 \times (XYZ) = 6$	2
Antennas	$2 \times (XYZ) = 6$	2
FTS pallet	$XYZ = 3$	1
O_2 subcarrier	$XYZ = 3$	1
N_2 subcarrier	$XYZ = 3$	1
O_2/N_2 tank	$XYZ = 3$	1
Berthing mechanisms	$3 \times (XYZ) = 9$	3
Total	326	74

average EI values of the nontarget modes and those of the target modes at the individual sensor units. The line on the figure represents the ratio of average ranks of the nontarget and target mode sets, i.e.,

$$\frac{\text{number of nontarget modes / number of sensor units}}{\text{number of target modes / number of sensor units}}$$

If the modal costs of the individual target and nontarget modes are the same, the sensor units below the line will observe more response from the target modes and the units above the line will observe more response from the nontarget modes. By removing the candidate sensor units above the line, the modal identification algorithm will not be influenced by excessive response measurement from the nontarget modes. In this example, however, the influence of the nontarget modes on the response at the measurement locations is expected to be insignificant due to the small modal cost of the nontarget modes. Thus, the removal of the units above the line from the candidate sensor units is considered unnecessary.

Using the best 133 sensor DOF, the 8 excitation DOF, and the 18 target modes, the generalized Hankel matrix in Eq. (22)

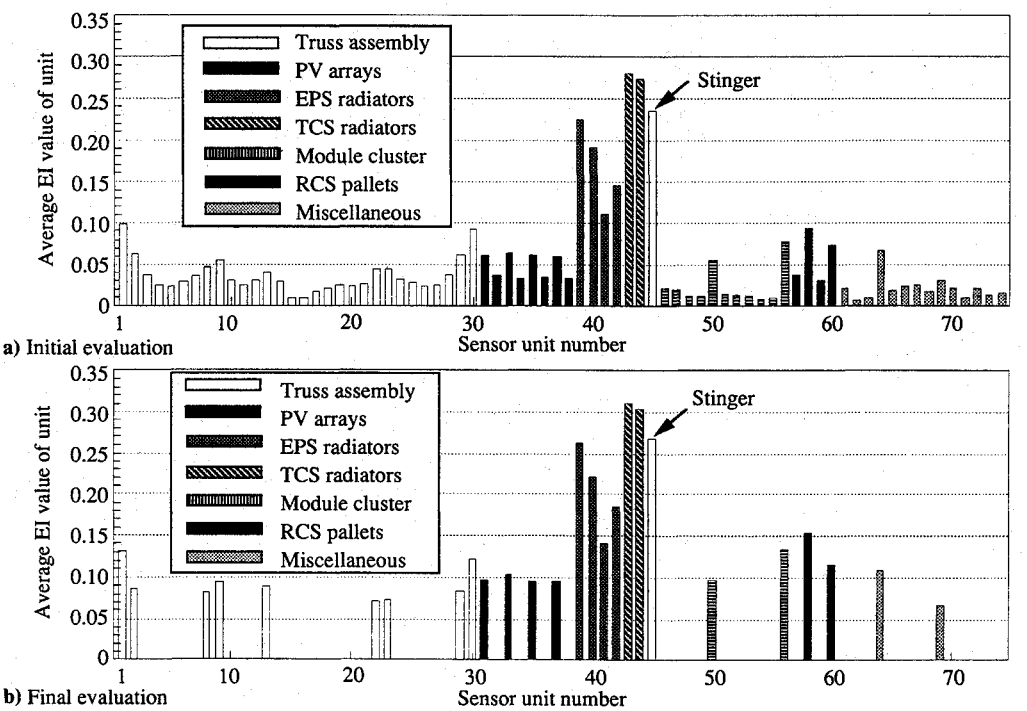

Fig. 4 Evaluation of average effective independence of the candidate sensor units.

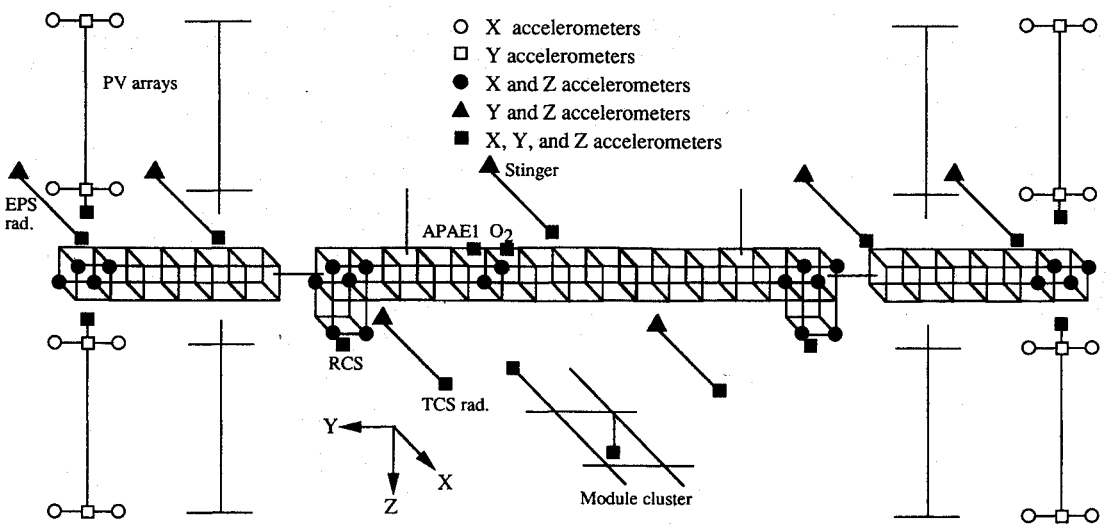

Fig. 5 Best locations for sensor placement.

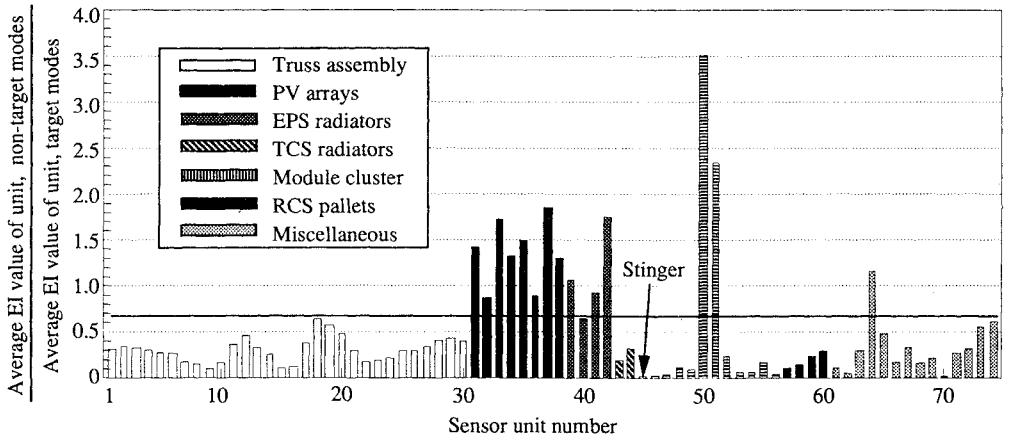

Fig. 6 Influence of nontarget modes on the EI distribution.

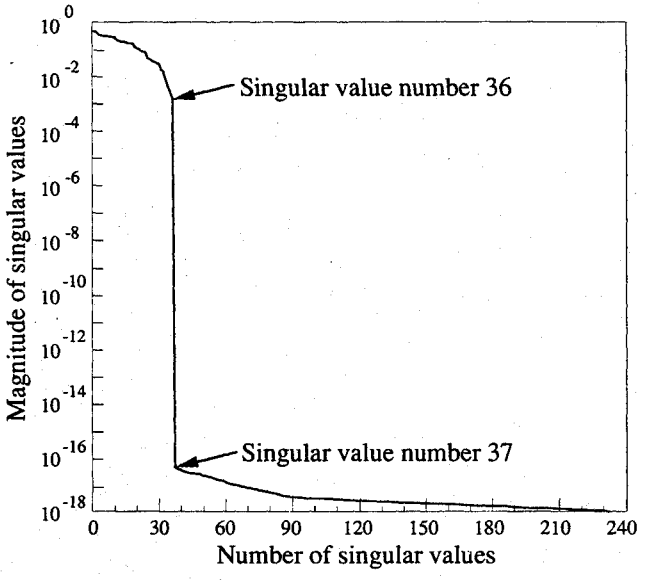

Fig. 7 Singular value distribution of the Hankel matrix using the best sensor locations.

was assembled, and the singular value distribution of the Hankel matrix was computed. The rank of the Hankel matrix should be 36 to ensure the identification of all 18 target modes. As depicted in Fig. 7, the singular value distribution shows a sharp drop after singular value number 36, indicating that there are 36 linearly independent vectors in the Hankel matrix. The condition number for the first 36 singular values is 304.6. The singular value distribution in Fig. 7 shows that all 18 target modes are identifiable using the 133 sensor DOF shown in Fig. 5.

Concluding Remarks

A systematic approach to placing accelerometers for on-orbit modal identification of large space structures was presented. The procedure examines the system and component modal cost of each mode to select target modes for modal testing and performs the sensor placement to enhance the modal identification of the target modes.

The correlation between sensor DOF selection and ERA performance was investigated. Although the investigation did not show what the absolute minimum number of sensors should be to identify all of the target modes, it was suggested that the number of sensors should be at least as many as the number of the target modes. The minimum number of sensors may also be influenced by other considerations of modal testing, such as compensation for the inaccuracy of an analytical model and the requirements for the correlation of analytical and measured modes and the finite element model improvement using modal test data.

Since the procedure depends on the analytical representation of the structure, the success of the approach will be influenced by the accuracy of the analytical prediction. Knowledge of the potential level of error on the analytical model would help obtain more robust sensor placement results.

Although the target modes in this study are selected to be global system modes, the component modal cost analysis provides versatility in selecting target modes for other purposes. If characterization of a component is of concern, the modes having the largest component modal cost corresponding to the component can be easily selected as target modes using the modal cost information. The sensors will then be placed to recover the target modes for the component.

Instead of evaluating individual sensor DOF, sensor placement based on the merits as a unit was proposed. Each unit is composed of several sensor DOF. This approach is beneficial in that extravehicular activity time and cost for sensor installation can be reduced and better understanding of individual components may be provided. The proposed procedure is systematic and computationally efficient. As an illustrative example, a sensor placement study for the MIE was presented.

Acknowledgments

This work is supported by NASA Langley Research Center Contract NAS1-19000. The help from Alan E. Stockwell and Lee-Hwa Chang of Lockheed Engineering and Sciences Company in calculating the component modal cost is acknowledged. The author also expresses his thanks to Kyong B. Lim of NASA Langley Research Center for providing helpful remarks on the sensor placement procedure.

References

[1]Raney, J. P., Cooper, P. A., and Johnson, J. W., "Space Station Freedom: Dynamic Instrumentation for a Large Space Structure," NASA TM-102711, Dec. 1990.

[2]Kim, H., and Doiron, H., "Modal Identification Experiment Design for Large Space Structures," AIAA Paper 91-1183, April 1991.

[3]Pappa, R. S., "Identification Challenges for Large Space Structures," *Sound and Vibration,* Vol. 24, No. 4, 1990, pp. 16-21.

[4]Blelloch, P., Engelhardt, C., and Hunt, D., "Simulation of On-Orbit Modal Tests of Large Space Structures," *Proceedings of the 18th Modal Analysis Conference,* Union College and Society for Experimental Mechanics, Vol. 2, Bethel, CT, 1990, pp. 926-932.

[5]Shah, P. C., and Udwadia, F. E., "A Methodology for Optimal Sensor Locations for Identification of Dynamic Systems," *Journal of Applied Mechanics,* Vol. 45, No. 3, 1978, pp. 188-196.

[6]Salama, M., Rose, T., and Garba J., "Optimal Placement of

Excitations and Sensors for Verification of Large Dynamic Systems," AIAA Paper 87-0782, April 1987.

[7]Kammer, D. C., "Sensor Placement for On-Orbit Modal Identification and Correlation of Large Space Structures," *Journal of Guidance, Control, and Dynamics,* Vol. 14, No. 2, 1991, pp. 252–259.

[8]Juang, J.-N., and Pappa, R. S., "An Eigensystem Realization Algorithm for Modal Parameter Identification and Model Reduction," *Journal of Guidance, Control, and Dynamics,* Vol. 8, No. 5, 1985, pp. 620–627.

[9]Skelton, R. E., Hughes, P. C., and Hablani, H. B., "Order Reduction for Models of Space Structures Using Modal Cost Analysis," *Journal of Guidance, Control, and Dynamics,* Vol. 5, No. 4, 1982, pp. 351–357.

[10]Feibish, R., "Dynamic Analysis NASTRAN Models of All Stages of the Reference Assembly Sequence Baseline (11/15/90)," Grumman Space Station Program, Space Station Engineering and Integration Contractor Memorandum, PSH-343-M090-174, Reston, VA, April 1990.

[11]Chen, C.-T., *Linear System Theory and Design,* Holt, Reinhart and Winston, New York, 1984, pp. 197–199.

Earl A. Thornton
Associate Editor